

A CHARACTERISTIC OF THE FLOW FIELD ON A HEATED ROTATING DISK

Yasuyuki Miwa¹, Noriyuki Furuichi¹ and Masaya Kumada¹

¹ Gifu Univ. 1-1 Yanagido Gifu, 501-1193, Japan, e-mail:furuichi@cc.gifu-u.ac.jp

Keywords: Mixed convection, Buoyancy, Centrifugal force, Velocity profile, Heated rotating disk, UVP

ABSTRACT

A velocity field on a heated rotating disk was obtained using UVP. The mean velocity on the heated flow field is obtained as a reasonable result and the effect of the heating can be observed near wall region. The unsteady flow field also shows clearly the effect of the heating by using a cross-correlation method. It was found from the variation of the cross-correlation coefficient that the region dominated by natural convection expands toward outside with increasing Grashof number.

1. INTRODUCTION

The purpose of this investigation is to study a flow structure on the heated rotating disk. The flow structure on the rotating disk (un-heated) has been studied by many researchers as it shows a typical flow transition scheme from laminar to turbulence. Moreover, a three-dimensional boundary layer appears as a spiral structure caused by the azimuthal velocity component induced by rotation and radial component by centrifugal force (*ex.* Littel and Eaton, 1994).

In the configuration of this paper, a heating of the disk is added. It is well known that this flow field exhibits a mixed convection, a field consisting of a forced convection induced by rotation and natural convection by buoyancy. It has been clarified well a mechanism of time-averaged heat transfer on the disk (Kreith et al. 1959), the vortex structure on the disk (Ogino et al., 1997) and turbulent heat flux (Elkins and Eaton, 2000). In this flow field, it is expected that the three-dimensional boundary layer is strongly affected by heating. A numerical simulation by Shingai and Kawamura (2002) reports, under the Ekman layer, an influence the heating in the means velocity filed. On the other hand, experimental reports about instability on the heated rotating disk are less, because of difficulty of the measurement. Since this flow field exhibits a three-dimensional boundary layer, as mentioned above, the measurement of the spatial distribution of the velocity is difficult by the visualization method like a PIV. The instabilities including the vortex structure as reported by Ogino et al. might be a function of the radial position. However, the radial variation of the unsteady structure has not been clarified quantitatively although the dependence of the rotating Reynolds and the Grashof number has been clarified.

In this study, we measure the velocity field by Ultrasonic Doppler method and show the vector mapping of the filed on the heated rotating disk for various Grashof number to confirm the correctly measurement under the field with temperature gradient. For unsteady flow structure, we consider it by the cross correlation of the velocity fluctuation.

2. EXPERIMENTAL APPARATUS AND COORDINATE SYSTEM

The schematic of the experimental apparatus and coordinate system are illustrated in Figure 1. A radius of the rotating disk submerged in the water tank (620×720×400mm) is $R=85\text{mm}$ and

a height of it is 60mm. A rotating speed of the disk was fixed on π (rad/s) (Rotating Reynolds number is $Re_\omega = R^2\omega/\nu = 2.27 \times 10^4$). A difference of the temperature between the rotating disk and water was varied $\Delta t = 0 \sim 35^\circ\text{C}$ as a parameter (Grashof number is $Gr = g\beta(T_w - T_\infty)R^3/\nu = 1.81 \times 10^7 \sim 4.21 \times 10^7$).

Three ultrasonic transducers (8MHz) were set for a vector field measurement with different angle and position as shown in Figure 1 (a) ((i)7, (ii)80, (iii)45 degree, respectively). Three beams were crossed at one point in the flow field to measure the velocity of three components. The arrangement of the transducers shown in Figure 1 (b) is for a measurement of an unsteady flow structure. Both transducers are set with inclination angle 7 degree. The velocity at the nearest point of the rotating wall was selected to compute cross-correlation coefficient. The measuring interval of the each transducer is 26msec. An error rate of the velocity was about 5% and position is 5% since a difference of density of water induced by the heating in this experiment.

3. RESULTS AND DISCUSSION

3.1 Mean velocity fields

Typical velocity profiles of the azimuthal component are shown in Figure 2. The velocity profile in a boundary layer is obtained clearly. These plots suggest a weak effect of the Grashof number. At $r/R=0.44$, the velocity profiles of heated case are slightly different with unheated case near disk region, especially $Gr=3.0 \times 10^7$. At $r/R=0.44$, although the trend of velocity profiles are almost similar, the velocity near wall region is the largest at $Gr=1.81 \times 10^7$. On the other hand, it should be noted that the velocity at $Gr=4.21 \times 10^7$ is almost similar with one of un-heated.

A typical velocity field of the r - z plane obtained in this experiment is shown in the Figure 3. The figure (a) shows an unheated case and the (b) shows the case that a difference of the temperature is 35°C ($Gr=4.21 \times 10^7$). In both cases, the cross-flow by the centrifugal force directed to outside of the disk can be observed clearly. This velocity component increases with increasing radial position. The flow directed toward the disk ($-z$) generating to take a balance of a flow rate with the cross-flow can be also observed. The difference of the flow field between figure (a) and (b) can be observed at the vicinity of the rotating disk. The cross-flow near wall of heated case is larger than unheated case since the density of the working fluid is changed by the heating.

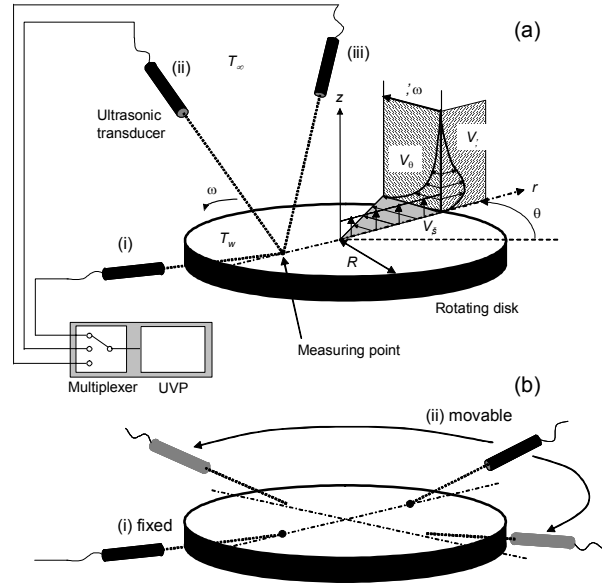


Figure 1. Schematic of the experimental apparatus and coordinate system

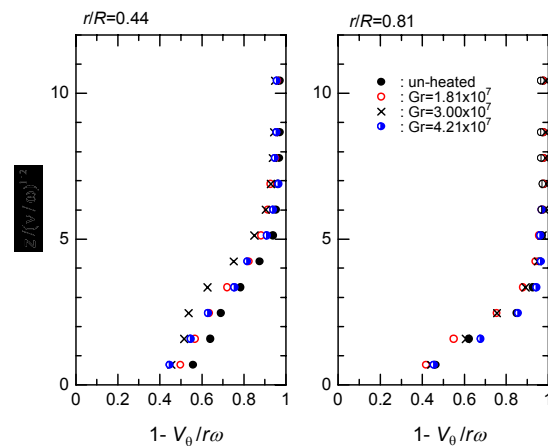


Figure 2. Examples of the velocity profile of azimuthal component

To observe detail of the velocity near wall region relating to the heating, the relationship between the cross-flow component V_r and wall normal component V_z is shown in Figure 4. Compared between $Gr=1.81 \times 10^7$ and unheated case, V_r component increases, however the trend of the relation of two components is almost same. With increasing Grashof number, the gradient of the line is decreases. This results shows that an appearance of an effect of the heating for small V_r component at the centre of the disk. When the cross-flow component is large at large radial position, the effect of the heating is small. Therefore, it is expected that the effectiveness of the heating is a function of the radial position.

To observe the effect of the heating to the three-dimensional boundary layer, the relationship between the azimuthal flow and cross-flow is shown in Figure 5. The plotted data is measured at $r/R=0.6-0.9$. To clear the trend of the plot, the lines are added. The clearly three-dimensional spiral structure is observed over the every condition and the effect of the heating. Especially, at the $Gr=4.21 \times 10^7$, the local peak exists near region of $1-V_\theta/r\omega=1$ comparison with other case. It shows that the wall normal position (z) of the maximum V_r velocity component is higher than other condition since large heating.

Thus, obtained velocity profile clearly shows the effect of the heating. These results might be reasonable one. It is concluded that the velocity under the field with small temperature gradient can be obtained correctly.

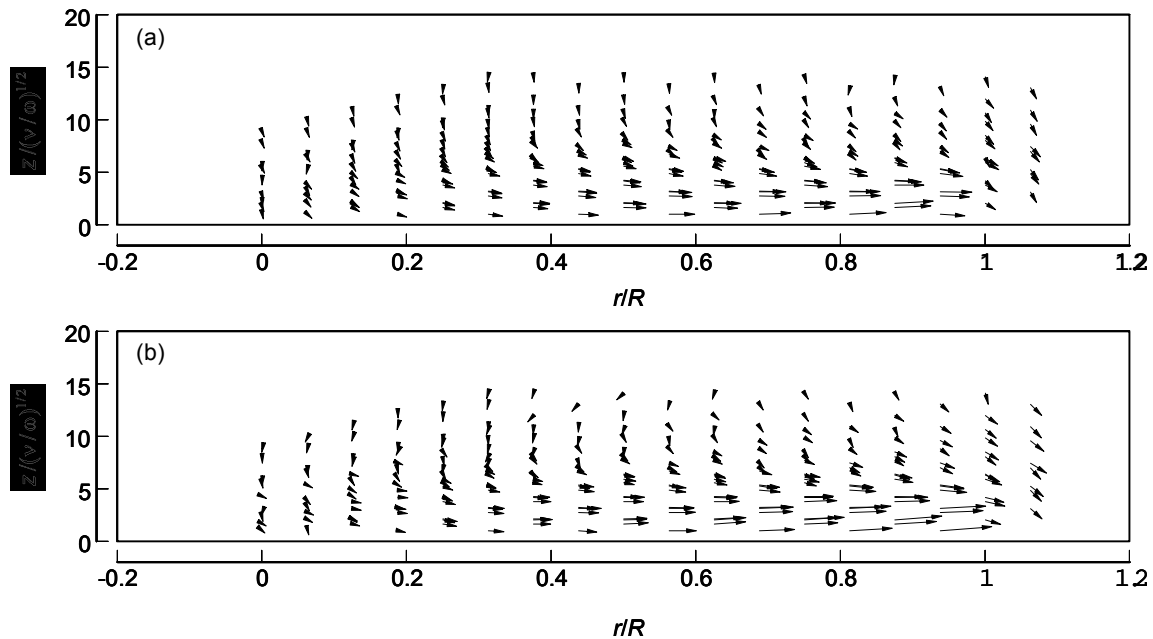


Figure 3. Examples of vector map at r - z plane (a) un-heated (b) $Gr=4.21 \times 10^7$

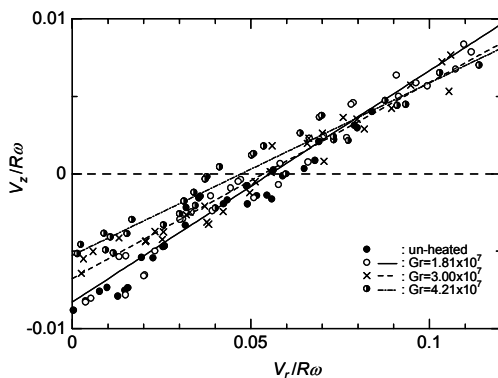


Figure 4. Relationship between V_r and V_z near wall region

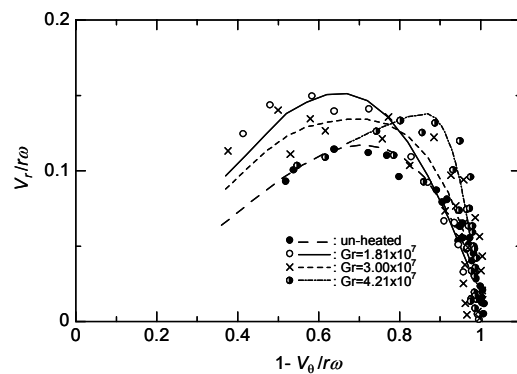


Figure 5. Polar plot of the velocity profile ($V_\theta - V_r$)

3.2 Correlation of the velocity fluctuation

The correlation coefficients of the velocity fluctuation of the radial component are obtained between the fixed and movable transducers. Azimuthal variations of the cross correlation coefficient $R_{vv}(r,r,0,\theta)$ are shown in Figure 6. The local minimums are observed at $\theta=\pi/2$ and maximums are $\theta=\pi$ at $Gr=1.81\times 10^7$. This behaviour of the correlation coefficient is similar at each radius positions and similar with unheated case although it is not shown in this paper. On the other hand, this behaviour is different largely with Figure (b); $Gr=4.21\times 10^7$. Especially, the $r/R<0.5$, the local minimum is observed at $\theta\approx\pi$.

Radial variation of $R_{vv}(r,r,0,\pi)$ is shown in Figure 7 to make an attention to the behaviour of it at $\theta=\pi$. The local maximums are observed at each Grashof number. These peaks move toward outside of the disk with increasing a Grashof number. The zero-cross points where the sign of the correlation coefficient changes minus to plus also move toward outside. At $r/R>0.7$, the correlation coefficient is almost same $R_{vv}\approx 0.2$ in every conditions. The correlation coefficient is a positive as shown the unheated case at $\theta=\pi$. Therefore, it is suggested that the forced convection is dominant $r/R>0.7$ at every case. It can be concluded that the region dominated by natural convection expands toward outside with increasing with Grashof number.

4. CONCLUSION REMARKS

The velocity field on the heated rotating disk was obtained using UVP. The mean velocity of the axial component on the heated flow field is obtained as a reasonable result and the effect of the heating can be observed near wall region. The UVP method can be applied to the measurement of flow field with small temperature gradient such as present field. The unsteady flow field also shows clearly the effect of the heating. The cross-correlation coefficient of the cross-flow component between each azimuthal angle varies with azimuthal and radial direction. It was found from the variation of the cross-correlation coefficient that the region dominated natural convection expands toward outside with increasing Gr number.

REFERENCES

- Elkins, C.J. and Eaton, J.K., J. Fluid Mech., 402, 2000, 225-253
 Kreith, F., Taylor, J.H. and Chong, J.P., ASME J. Heat Transfer, 1959, 95-105
 Littell, H.S. and Eaton, J.K., J. Fluid Mech. 266, 1994, 175-207
 Ogino, F., Saito, Y., Yoshida, T., Masuda, K. and Mizuta, K., J. Chemical Eng. 23, 5, 1997, 679-686 (in Japanese)
 Shingai, K. and Kawamura, H., Thermal Science and Engineering, 20, 1, 2002, 25-33

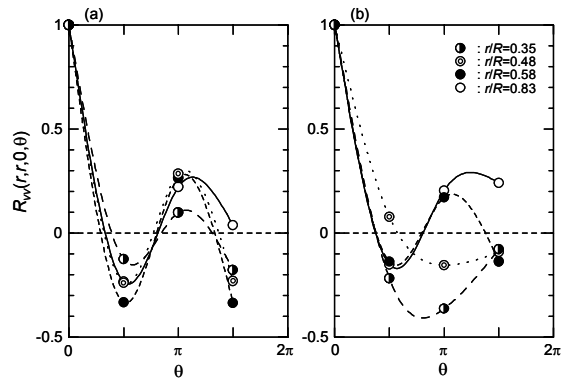


Figure 6. Azimuthal variations of the correlation coefficient (a) $Gr = 1.81 \times 10^7$ (b) $Gr = 4.21 \times 10^7$

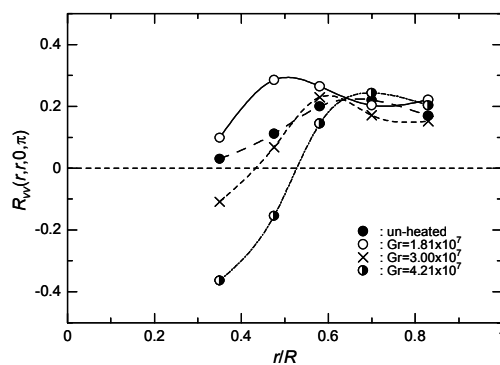


Figure 7. Radial variations of the correlation coefficient